

Development of bearings and a damper based on magnetically controllable fluids

This article has been downloaded from IOPscience. Please scroll down to see the full text article.

2006 J. Phys.: Condens. Matter 18 S2959

(<http://iopscience.iop.org/0953-8984/18/38/S29>)

View [the table of contents for this issue](#), or go to the [journal homepage](#) for more

Download details:

IP Address: 129.252.86.83

The article was downloaded on 28/05/2010 at 13:50

Please note that [terms and conditions apply](#).

Development of bearings and a damper based on magnetically controllable fluids

J M Guldbakke and J Hesselbach

Institute of Machine Tools and Production Technology, TU Braunschweig, Langer Kamp 19b,
38106 Braunschweig, Germany

E-mail: j-m.guldbakke@tu-bs.de

Received 28 April 2006, in final form 14 July 2006

Published 8 September 2006

Online at stacks.iop.org/JPhysCM/18/S2959

Abstract

This paper presents two different kinds of magnetically controllable fluid bearings and a new magnetorheological fluid damper based upon open porous metallic foams. For the bearings, it will distinguish between a magnetohydrostatic bearing and a hydrostatic bearing with a magnetically controllable fluid. The magnetohydrostatic bearings get their load bearing capacity from the magnetohydrostatic pressure that is generated by the gradient of the magnetic field along a fluid surface. With such magnetohydrostatic bearings a specific load up to 1.6 N cm^2 can be reached. To support heavier loads hydrostatic bearings with magnetically controllable fluids can be used. This bearing concept makes it possible to achieve a constant bearing gap even if the load of the bearing changes. For this purpose the fluids are used as a hydraulic medium. Due to the magnetically controlled rheological behaviour of the fluid the bearing gap remains constant. The great advantage of this closed loop system compared to that of common hydrostatic bearings using valves is the quicker response to payload changes. The reason for that is that the active element (i.e. the fluid) acts directly inside the bearing gap and not outside like in the case of valves. The foam damper developed uses the fluid to produce controllable damping forces. The open porous foam is directly placed in the active volume of the damper. By moving the foam piston the magnetically controllable fluid is pressed through the pores. The flow in the pores can be controlled by changing the fluid viscosity by applying a magnetic field. With this damper structure it is possible to reach higher damping forces whilst featuring a small design space.

1. Introduction

Semi-active devices have received significant attention in recent years because they offer the adaptability of active control devices without requiring the usually associated large power

sources. Bearings and dampers based on magnetically controllable fluids are such semi-active devices. They change fluid properties to control load capacity and controllable damping forces respectively.

Two different bearing principles with magnetic fluids will be introduced in this paper. The first is the magnetohydrostatic bearing principle with magnetically controllable fluid. These bearings get their load capacity from the hydrostatic pressure produced by an external pump. Due to the fact that these fluids change their rheological properties with the change of an external magnetic field it is possible to achieve a constant bearing gap when the payload changes. The second demonstrator developed is a magnetohydrostatic bearing. This type uses the magnetic pressure inside a ferrofluid that arises from a magnetic field. The magnetorheological fluid damper developed consists of an open porous foam piston. This piston is directly placed inside the active volume of the damper. The fluid is pressed through the pores when the piston moves. By changing the magnetic field the fluid viscosity can be influenced and thus the flow rate can be controlled.

In the following sections the principle of both bearings and the foam damper will be explained. Further on the set-up and measurement results of each demonstrator will be described and a conclusion is drawn. The last section gives an overall summary and a short outlook.

2. Hydrostatic bearings with magnetic fluids

2.1. Principle of hydrostatic bearings

Hydrostatic bearings are an established technology in the field of machine tools. A conventional hydrostatic bearing consists of two sliding surfaces that are separated by a thin oil film. The oil is pressed with a constant flow rate Q by an external pump through the evolving gap. In figure 1 this principle is shown. To maximize the bearing force one sliding surface has a special topology: the depth of the pad is much bigger than the depth of the land. Thus the pressure inside the pad is constant and declines to the ambient pressure along the land. The resulting pressure distribution and the load remain in the equilibrium state. If the oil flow rate and the load are staying constant, the gap h is constant. The bearing force depends only on the pressure in the pad p_t and the effective pad area A_{eff} .

$$F(Q) = p_t(Q) \cdot A_{\text{eff}}. \quad (1)$$

The effective pad area is larger than the physical pad size because a part of the land contributes to the bearing force. Assuming a linear decrease of the pressure along the land, the mean value of the pressure inside the land is $\frac{1}{2} p_t$. To calculate $p_t(Q)$ some calculations are needed. For Newtonian fluids which are used in conventional devices this is well known (κ = viscosity) [1, 2]:

$$F(Q) = \frac{12 \cdot l_s \cdot \kappa \cdot Q}{b_t \cdot h^3} \cdot A_{\text{eff}}. \quad (2)$$

This equation shows the main challenge of a conventional hydrostatic bearing: if the load F changes, the flow rate Q needs to be changed in order to achieve a constant bearing gap h . This flow rate change is usually realized by external mechanical valves. Because of the poor dynamics of these valves the time of response to load change is long. Therefore the stiffness of hydrostatic bearings is limited.

However, magnetorheological (MR) fluids exposed to a magnetic field B do not behave like Newtonian fluids. Due to the fact that magnetically controllable fluids change their rheological properties under the influence of a magnetic field, it is possible to control a constant gap without

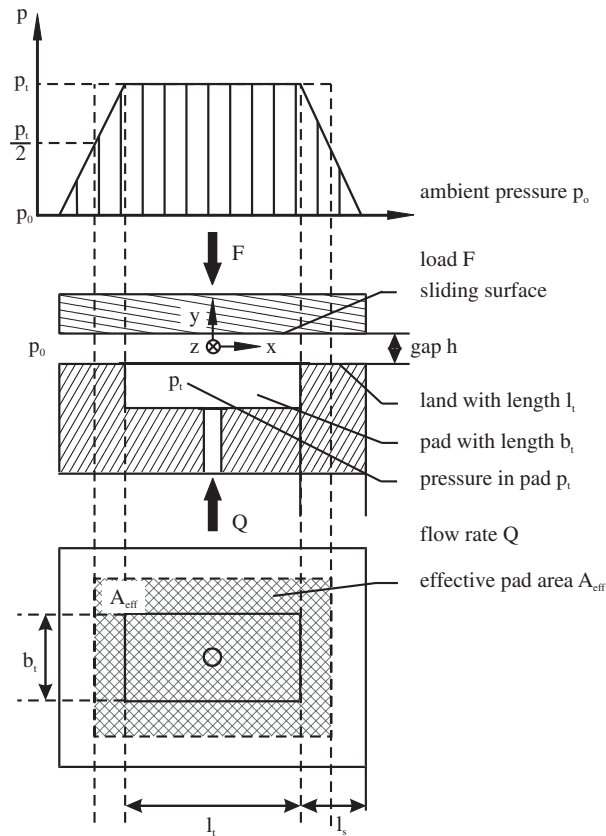


Figure 1. Principle of the hydrostatic bearing.

changing the flow rate. To calculate this behaviour some characteristics of the rheological behaviour of magnetic fluids need to be taken into account. A widely used description for stress behaviour of MR fluids is the so-called Bingham model (τ_0 : shear stress, D_s : shear rate) [3]:

$$\tau(B) = \tau_0(B) + \kappa \cdot D_s \quad (3)$$

With regard to the Bingham model, (3) leads to an implicit equation for $p_t = p_t(h, b_t, l_s, Q, \tau_0, \kappa)$:

$$0 = \underbrace{(b_t \cdot h^3)}_a \cdot p_t^3 + \underbrace{(3 \cdot l_s \cdot \tau_0 \cdot b_t \cdot h^2 + 12 \cdot l_s \cdot \kappa \cdot Q)}_b \cdot p_t^2 + \underbrace{(5 \cdot b_t \cdot l_s^3 \cdot \tau_0^3)}_c \quad (4)$$

An estimation with reasonable values for geometrical and fluid properties shows that the term c is negligible. Resolving equation (1) leads to [4]

$$F(Q, B, h) = \left(\underbrace{\frac{3 \cdot l_s \cdot \tau(B)}{h}}_{\text{Bingham}} + \underbrace{\frac{12 \cdot l_s \cdot \kappa \cdot Q}{b_t \cdot h^3}}_{\text{Newtonian}} \right) \cdot A_{\text{eff}} \quad (5)$$

This equation shows the advantage of hydrostatic bearings with magnetorheological fluids over conventional designs: if the payload F changes it is possible to change the flow rate Q , if the

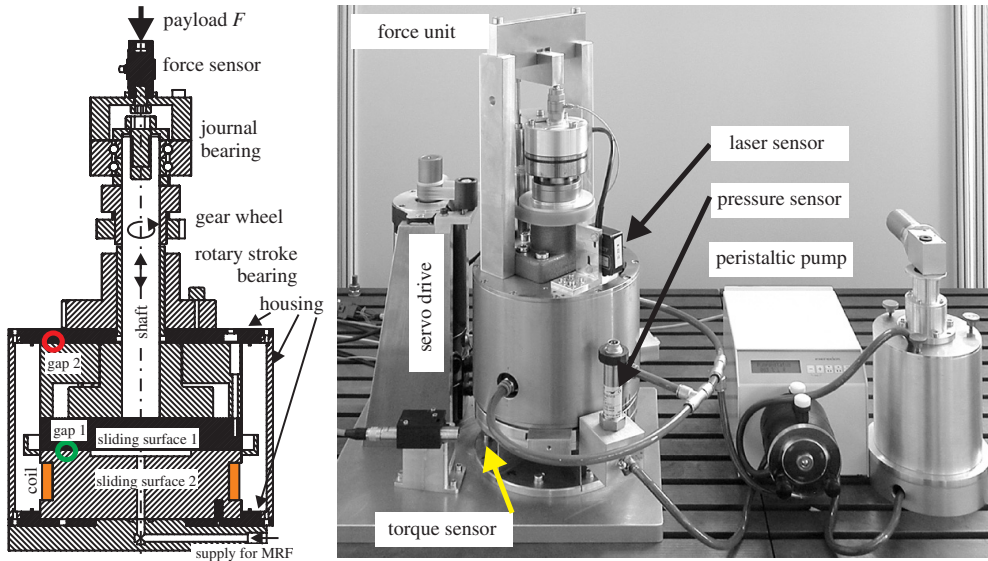


Figure 2. Sectional view and photograph of the hydrostatic bearing with magnetic fluids [5].
(This figure is in colour only in the electronic version)

gap h is constant. With the magnetorheological fluid inside the gap a change of the magnetic field can be used to control the bearing gap.

A quality characteristic factor Γ (control ratio) of this bearing concept is the payload range that can be supported without a change of the gap.

$$\Gamma = \frac{F(\tau_{0,\max})}{F(\tau_0 = 0)} = \frac{\tau_{0,\max} \cdot b_t \cdot h^2}{4 \cdot \kappa \cdot Q} \quad (6)$$

where $h(B = 0) = h(B = B_{\max}) = \text{const}$.

As can be seen, a large gap h leads to a wide payload range. In conventional hydrostatic bearings the stiffness is proportional to h^{-4} . Therefore it is necessary to make the gap as small as possible. Consequently the sliding surfaces must have narrow tolerance limits.

2.2. Experimental set-up and results

To verify the concept of hydrostatic bearings with magnetically controllable fluids a test rig was set up. Aiming at a simple realization a thrust bearing was chosen for the experimental set-up (figure 2). The two sliding surfaces are separated by a small gap of about $300 \mu\text{m}$ (gap 1) and have a diameter of 160 mm. The pad has a diameter of 54 mm. The coil (100 windings, 1Ω) for generating the magnetic field and the supply of the fluid is placed in the frame. The sliding surface 1 can rotate and move vertically; other degrees of freedom are blocked by a rotary stroke bearing. The rotation is generated by an external servo-motor and transmitted by a toothed belt and a set of gears. To generate dynamic payloads of up to 300 N a piezo-stack is attached. A journal bearing is used to decouple the rotation of the shaft from the load unit. A peristaltic pump is utilized too in order to generate the desired flow rate ($0.01\text{--}0.8 \text{ l min}^{-1}$). This type of pump was chosen to prevent the magnetically controllable fluid from being polluted by abrasion and the lubricant of the pump. The maximum pressure of this pump is 3 bar. To measure the change of the gap a laser triangular measurement system with a resolution of $1 \mu\text{m}$ is used. Further on a torque sensor is placed under the bearing to measure

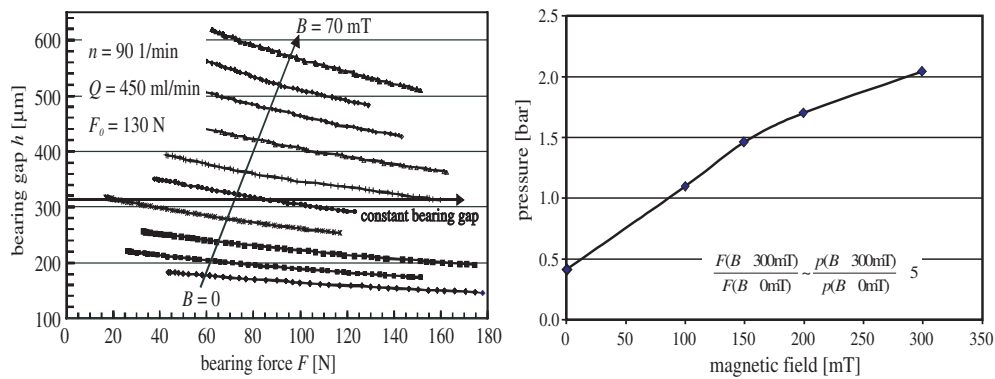


Figure 3. Left: measurement of the bearing gap change with the bearing force for different magnetic fields [6]; right: FEA of the bearing force capacity for a hydrostatic bearing with NMRF [7].

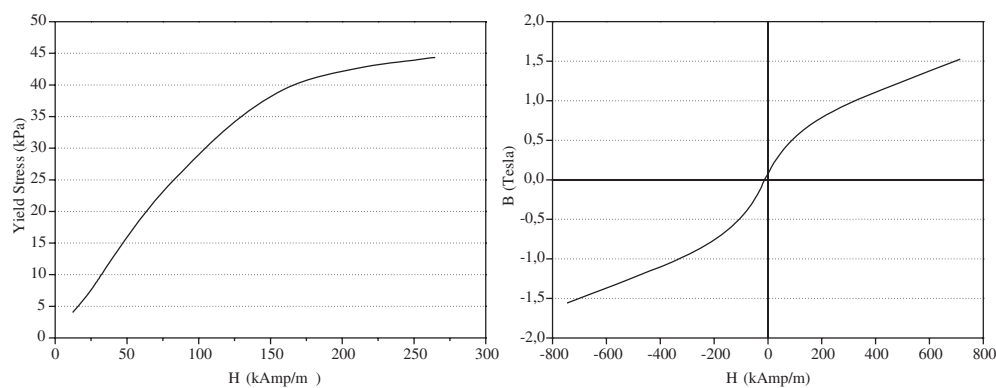


Figure 4. Yield stress versus magnetic induction (left) and the magnetization curve of MRF132-AD fluid (right) [8].

the torque that is transmitted by the bearing. The housing of the device is made of standard magnetic steel to guarantee optimal transmission of the magnetic field. Sliding surface 2 is bonded with a CFK plate. In this plate two magnetic field sensors are integrated. Therefore, the magnetic gap is about 1 mm wider than the fluid gap. Nevertheless the magnetic field can be assumed to be homogeneous and nearly constant over the whole gap. All measurements were made with a commercially available MR fluid (MRF132-AD, Lord Cooperation, particle size $\approx 2\text{--}20$ μm , carrier liquid = hydrocarbon, now replaced by MRF-132DG).

To prove the principle the gap force dependences for different magnetic fields were measured (figure 3 (left)). The measurements were carried out with a constant flow rate and a constant angular velocity of the bearing (90 turns per minute). First of all it can be seen that the gap change due to load changes decreases when the gap size falls. This is a known behaviour of hydrostatic bearings; thus the gap normally is chosen as small as possible. Furthermore the measurement shows that a constant bearing gap can be achieved if the magnetic field increases with the load. The required magnetic field is very low (< 100 mT) compared to the capabilities of the magnetic fluid used which are limited by the magnetic saturation (see figure 4). In other words: the full potential of the MR fluid used is not tapped by this application. Therefore, finite element analysis took place to investigate whether another class of magnetically controllable

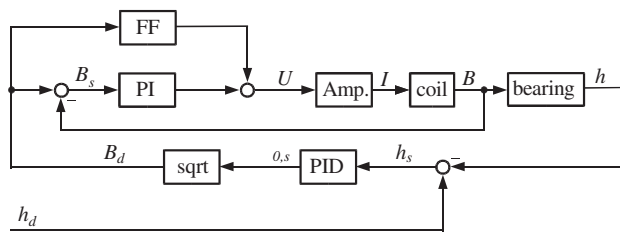


Figure 5. Control circuit for a hydrostatic bearing.

fluids, so-called nanomagnetorheological fluids (NMRF), provide enough magnetorheological effect for the usage in this application. These fluids contain much smaller particles (~ 30 nm). This results in a weaker magnetorheological effect; on the other hand the sedimentation stability of these fluids is higher. Further on the small particles allow smaller bearing gaps which is important for the inherent stiffness of the bearing.

Figure 3 (right) shows a finite element analysis of a hydrostatic bearing with a nanomagnetorheological fluid (BASF, 2800/93/132-1, particle size ~ 30 nm, carrier liquid = alcohol). Because the bearing force is proportional to the pressure it can be derived from this simulation that the maximum bearing force is 5 times higher than the minimum bearing force without any change in the bearing gap. This demonstrates that a hydrostatic bearing with nanomagnetorheological fluid is sensible.

2.3. Closed loop control of hydrostatic bearings

To control the bearing gap a cascaded control approach was chosen (figure 5). The inner cascade controls the magnetic field. To improve the dynamic behaviour of the magnetic field a feedforward term is used (FF). The dynamic behaviour of the magnetic field is mainly limited by the maximum voltage which is available from the power supply (24 V). A PI controller turned out to be the simplest algorithm which is able to counteract the hysteresis of the magnetic field. The gap controller was realized as a PID controller in the outer loop.

Figure 6 compares the system responses of the open loop system and the closed control loop to a load change. Without control the applied load change of about 160 N leads to a gap change of about $150 \mu\text{m}$. The overshoot of the force is produced by the piezo-stack, because the initially high force reduces according to the yield of the bearing. Changing the load acting on the controlled system by 320 N causes a dynamic gap change of only $15 \mu\text{m}$. The control error is eliminated in about one second. This time is necessary for refilling the decreased gap with fluid. Due to the constant flow rate this time cannot be shortened. Comparing the two systems it is obvious that the dynamic stiffness of the bearing is significantly improved. After reaching the equilibrium state the bearing has an infinite stiffness.

2.4. Conclusion and outlook

The concept of a hydrostatic bearing was realized and it was shown that with a suitable control a quasi-infinite stiffness could be achieved. Results from simulations recommend using magnetically controllable fluids with much smaller particles. This will allow bearing gaps that are comparable to gaps used in contemporary commercial hydrostatic bearings. Overall the advantages of the hydrostatic bearings with magnetic fluids can be summarized as follows:

- (i) The load bearing capacity is significantly higher compared to those for bearings based on the magnetic pressure [9].

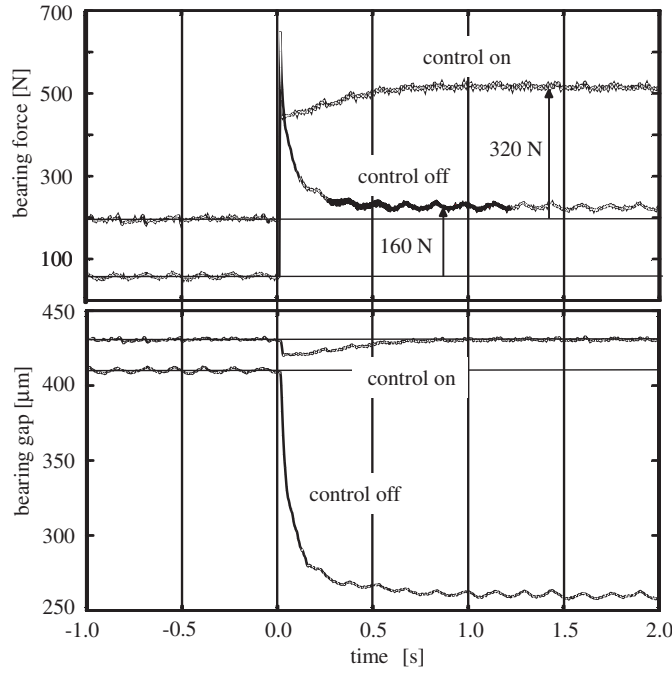


Figure 6. Control characteristic of the hydrostatic bearing.

- (ii) Because the fluid flows through the device it is possible to use standard magnetically controllable fluids (no problems with settlement).
- (iii) The actuator for controlling the bearing gap resides directly inside the gap. This leads to an outperforming timing characteristic.
- (iv) Conventional hydrostatic bearings need a gap size as small as possible to achieve a good stiffness. Hydrostatic bearings with magnetically controllable fluids can achieve nearly infinite stiffness with moderate gap sizes. Therefore the planarity of the sliding surfaces is not so critical.

3. Magneto-hydrostatic bearings

3.1. Principle of magneto-hydrostatic bearings

Magneto-hydrostatic bearings get their load bearing capacity from the magneto-hydrostatic pressure that is produced by the gradient of a magnetic field at the fluid surface of a magnetic fluid. This can be described by the main equation of hydrostatics:

$$\nabla p = \rho \cdot \vec{g} + \mu_0 \cdot M \nabla H. \quad (7)$$

An estimation of payloads which can be directly generated with the use of the magneto-hydrostatic effect is given by Berkovsky [9]: in the case where the magnetically controllable fluid is completely saturated, the maximum payload F_{\max} of the bearing can be calculated using

$$F_{\max} = \mu_0 \cdot M_{fs} \cdot H_s \cdot A. \quad (8)$$

- M_{fs} is the saturation magnetization of the fluid.

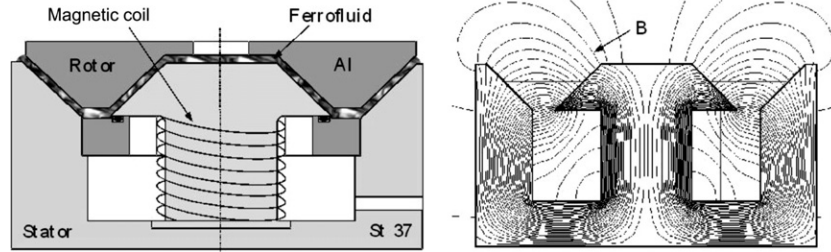


Figure 7. Experimental set-up of an axial magneto-hydrostatic bearing (left) and magnetic field distribution in the bearing without magnetic fluid (right).

- H_s is the magnetic force at the interface between the fluid and the bearing area.
- A is the bearing area.

Therefore the specific payload $f = F/A$ is

$$f = \mu_0 \cdot M_{fs} \cdot H_s. \quad (9)$$

Deploying characteristic magnitudes for $M_{fs} = 5 \times 10^5 \text{ A m}^{-1}$ and for $H_s = 1.5 \times 10^5 \text{ A m}^{-1}$ the specific bearing capacity is of the order of 1 N cm^{-2} . In comparison to those for conventional hydrostatic bearings the specific load is smaller. But an advantage of these bearings is that the stability of the bearing system can be guaranteed without the use of a control loop.

With equation (8) only a rough estimation of the achievable load capacity is possible. Because the payload is exclusively dependent on the magnetic field distribution inside the bearing, the use of a finite element method is recommended. The initial conditions are given by the magnetizing curves of the fluid and the guidance material as well as the geometry of the bearing. With these values it is possible to compute the distribution of the magnetic field. With the following equation the magneto-hydrostatic pressure at the fluid surface can be calculated. For the calculation only the direction (y component) of the payload must be considered for the magnetizing force H_g and the magnetization of the fluid at the interface between the fluid and rotor bearing area [7]:

$$p_m = \mu_0 \cdot M_{gy} \cdot H_{gy}. \quad (10)$$

The integration of the pressure over the whole bearing area delivers the bearing capacity.

3.1.1. Experimental set-up and results. In figure 7 the experimental set-up of an axial magneto-hydrostatic bearing is shown. This arrangement consists of three elements: a magnetic field source (stator), a magnetically controllable fluid and a non-magnetic rotor. The coil wound around the ferromagnetic stator generates a magnetic field in the trapeze shaped slot which represents the bearing area. The lower area of the slot consists of a paramagnetic ring (Al). The coil has 298 windings and a resistance of 1Ω . Massive steel (St 37) is used for all ferromagnetic parts of the experimental set-up. The rotor consists of paramagnetic aluminium. Figure 8 shows pictures of the axial magneto-hydrostatic bearing.

In the enlarged section it is visible that on the edge a strong magnetic field exists. The ferrofluid generates a corona of Rosensweig instabilities.

For bearing gap measurements a laser triangulation sensor is mounted. As a force sensor a resistance strain gauge with a nominal force of 100 N is used for force measurement. The results of the measurements and the FEM simulations of the magneto-hydrostatic force distribution

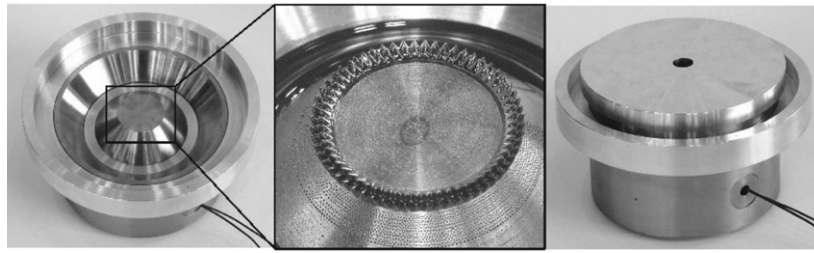


Figure 8. Pictures of the axial magneto-hydrostatic bearing: stator (left), section enlargement of the stator with ferrofluid (middle) and general view of the bearing (right).

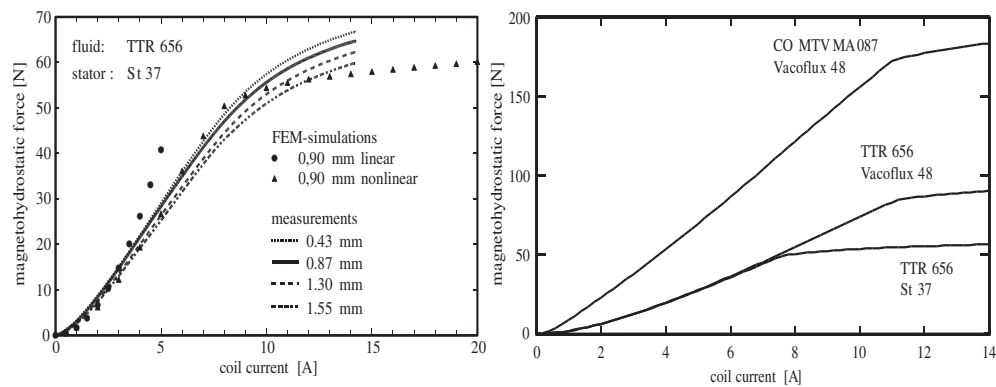


Figure 9. Comparison of FEM simulations and measurement results (left) and FEM simulations of the load bearing capacity for different combinations of magnetic fluids and stator materials (right).

over the coil current are shown in figure 9. As the magnetic fluid a ferrite based ferrofluid (TTR 656, particle size ~ 11 nm, carrier liquid = TR-30) with a saturation of 60.3 mT was used. The diagram of the magnetohydrostatic force versus the coil current can be split into three sections. In the left section from 0 to approximately 3 A the curve shows a squarish increase that merges into a linear progression in the middle section, from approximately 3 to 10 A. In the right section the force seems to converge to an upper limit. The shape of the curve may be explained using equation (10): for weak magnetic fields the magnetization of the ferrofluid is increasing linearly with the magnetization force H_g . Further on the magnetization force increases linearly with the coil current as long as the magnetic material of the stator does not approach its saturation magnetization. This explains the squarish increase of the curve in the left part of the diagram. For stronger magnetization forces the ferrofluid reaches its saturated state and therefore remains constant. The magnetohydrostatic pressure rises only linearly with the magnetic field and therefore with the current. In the right section where higher coil currents were applied the magnetic material of the stator is saturated, too. The consequence is that the stator represents a rising magnetic resistance, whereby the rate of the stray fields, which are not acting in the bearing gap, is strongly increasing. The conclusion is that the magnetohydrostatic pressure and, therefore, the magnetohydrostatic force remain constant. The shown FEM simulation with the nonlinear magnetization curve of the ferrofluid and stator material used fits the measurements in an acceptable way. For this reason FEM simulations can be used as a suitable tool for estimating the potential of magneto-hydrostatic bearings.

In figure 9 (right side) results from FEM simulations where the load bearing capacity for various combinations of magnetic fluids and stator materials were simulated are shown. Using a highly permeable iron–cobalt alloy with a saturation magnetization of 2.35 T (Vacoflux 48) instead of St 37 would increase the load capacity from 60 to 80 N. A cobalt based ferrofluid (CO MTV MA 087, MPI Mühlheim, particle size ~ 9 nm, carrier liquid = kerosene) with a saturation magnetization of 100 mT would additionally increase the load bearing capacity to even 180 N. Dividing this value by the bearing area of 113 cm^2 the resulting specific load capacity can be assumed to be approximately 1.6 N cm^{-2} .

3.2. Conclusion and outlook

The demonstrator which is introduced in this paper shows that the idea of using magnetic fluids in a hydrostatic bearing is technically feasible and offers the potential for various applications. Finite element methods were used in order to investigate load capacity optimizations. As a result it was found out that the achievable load capacity is expected to be 1.6 N cm^{-2} . Even higher bearing capacities may be possible by using advanced bearing geometries. Validations with the experimental data proved that FEM simulations provide reliable results for these tasks. By changing the inclined stator area geometries, a more constant magnetic field distribution along the bearing areas can be realized. This would cause a more constant magnetization and therefore a higher payload. Another possibility for increasing the bearing capacities would be the development of new ferrofluids with a higher saturation limit. This would be feasible either by increasing the concentration of cobalt ferrofluids or the use of particle materials with higher magnetization saturation.

4. Magnetorheological fluid damper

4.1. Principles of magnetorheological fluid dampers

At present the most important commercial application of magnetically controllable fluids is in dampers. In recent years magnetorheological (MR) dampers went into series production. For example the company Cadillac uses them to equip their cars [10]. For the operating mode of these dampers three principles according to the three flow types (shear, flow and squeeze mode) are known. The most common principle uses the shear mode where a fluid volume inside a magnetic coil is sheared by the movement of the damper. Applying a magnetic field to this fluid makes it possible to control the dynamic properties with the yield stress, which is dependent on the magnetic field. The achievable damping force can be described as a sum of a weak magnetic field dependent viscous component F_η and a strong field dependent component F_τ [11]:

$$F(B) = F_\eta + F_\tau(B) = \frac{\eta(b) \cdot v \cdot A}{h} + \tau_0(B) \cdot A. \quad (11)$$

- B : magnetic field;
- η : Bingham viscosity;
- τ_0 : shear stress;
- A : shear area;
- h : distance between the shear areas;
- v : relative velocity of shear areas.

The control range of these dampers is defined as the ratio V between the damping forces without and with the maximum magnetic field:

$$V = \frac{F(B_{\max})}{F_0} = 1 + \frac{h}{v} \cdot \frac{\tau_{0,\max}}{\eta_B}. \quad (12)$$

A wide control range in conventionally designed dampers can be realized with a large gap h between the piston and cylinder. However this implies some disadvantages:

- More fluid will be needed (higher costs and weight).
- A higher volume must be pervaded by the magnetic field. Therefore more energy will be needed to generate the magnetic field.
- The package size of the damper will increase.
- The achievable damping forces decreases.

Another possibility for getting a wide control range for the damper is the use of a fluid with increased magnetorheological effect (maximum shear stress). Such an ideal fluid consists of large particles of highly permeable material. The disadvantage of this ideal fluid arises from sedimentation processes of the particles which will lead to inhomogeneous properties of the fluid. In the following a new damping concept will be presented that allows a highly active damping volume in combination with a high achievable damping force as well as a small design space.

4.2. Magnetorheological fluid foam damper

The basic idea of this new kind of damper is based on open porous foams. Over the last decade these metallic foams have been established as a new material for various purposes. The main advantage of these foams is a high stability combined with a low weight. For magnetorheological applications especially, the open porosity is important: the metallic foam can be directly placed into the active volume of the damper in a magnetic fluid. For system modelling in a first approximation the foam may be considered as an additional rheological resistance. Hence, the achievable damping forces can be shifted to higher values. The open porosity of the foam is another independent design parameter which can be used to optimize the achievable damping forces. Figure 10 shows the principle of a magnetorheological fluid foam damper. The piston consists of an open porous metallic foam and is located inside a magnetic coil. Moving this foam piston presses the magnetic fluid through the pores of the foam. The flow in the pores can be controlled by changing the viscosity of the fluid by applying a magnetic field. Additionally, the damping force can be adjusted by the use of different open porous metallic foams. Figure 11 shows a magnetorheological fluid foam damper that was developed and built by the IWF [13]. The metallic foam used consists of a bronze alloy with an open porosity of 10 ppi (pores per inch). As a filling for the damper a magnetorheological fluid from the company Lord (MRF-132AD, particle size $\approx 2\text{--}20 \mu\text{m}$, carrier liquid = oil) was chosen. The advantages of this magnetorheological fluid damper based on open porous metallic foams over conventional MRF dampers are:

- Higher active volume in combination with a more compact design space.
- Wider range of control of the damping force.
- Better concentration of the magnetic field in the core, and therefore a high degree of efficiency from magnetic field generation.
- The range of the controllable damping force can be shifted by using different open porous metallic foams.

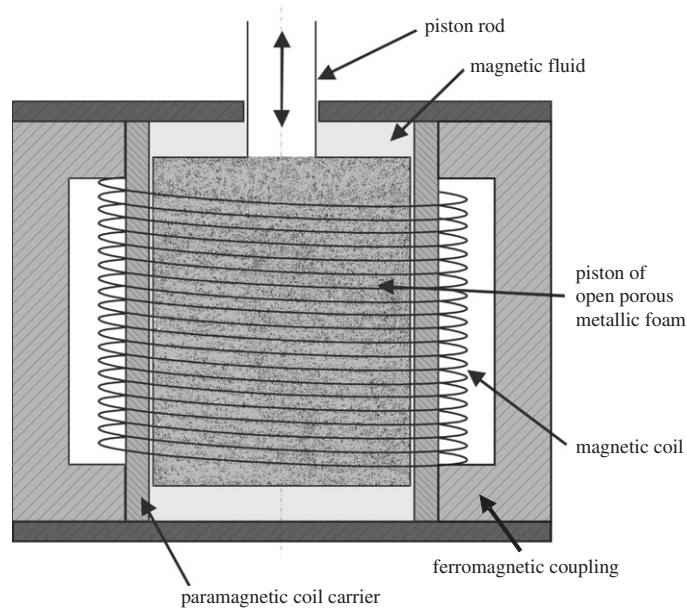


Figure 10. Principle of the foam damper [12].



Figure 11. Picture of the magnetic fluid damper (left) and the foam piston (right).

4.3. Experimental set-up and results

To carry out experiments a test rig was set-up; this is shown in figure 12. The excitation of the magnetorheological damper is done with an electromagnetic shaker. With this shaker a stroke of 13 mm and a maximum force of 445 N can be generated. To drive the shaker an additional power amplifier is required. The amplifier is connected to the shaker and to a signal generator. For position measurement an inductive position sensor from the company HBM is used. A piezoelectric sensor mounted between the damper and shaker measures the damping force. The acquisition of the measurement data is done with the MATLAB/XPC-Target package.

To find basic damper properties repeated test sequences were carried out. Therefore currents from 0 to 3 A were applied to the coil inside the damper. With the signal generator a sinusoidal oscillation is generated. The frequencies of this oscillation are between 3 and 10 Hz. As an example, figure 13 (left side) shows experimental data which were obtained at an excitation frequency of 10 Hz and an ambient temperature of 20 °C. In this figure the displacement versus the force is shown for currents between 0 and 2.5 A. It can be seen that

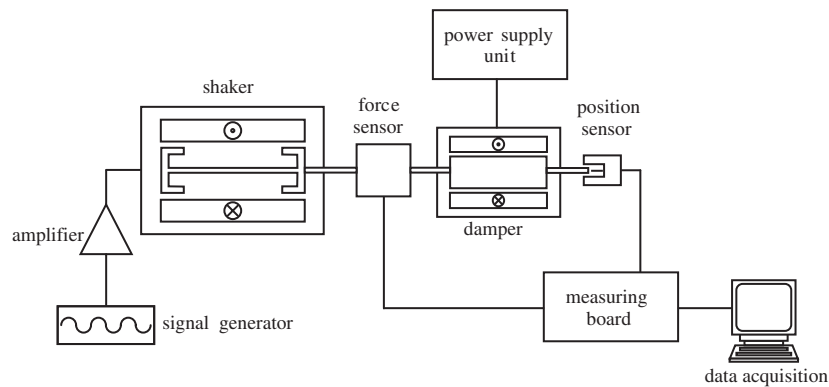


Figure 12. Experimental set-up.

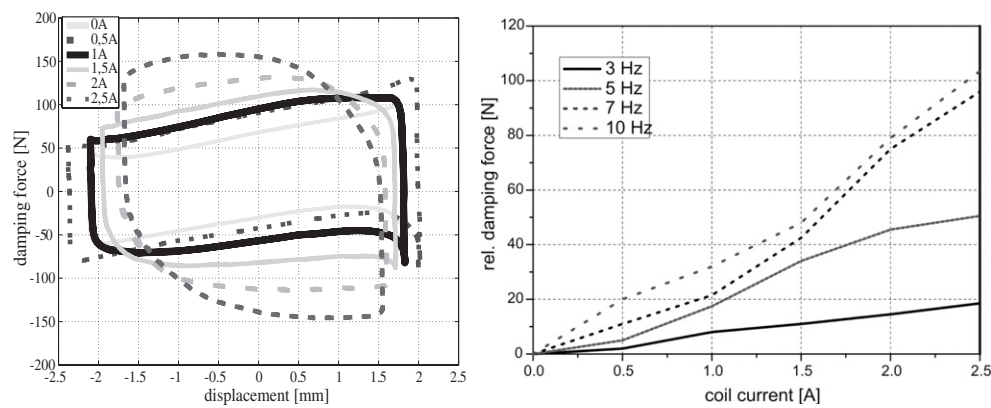


Figure 13. Damping force as a function of displacement ($I = 0\text{--}2.5\text{ A}$, $T = 20^\circ\text{C}$, $f = 10\text{ Hz}$) (left) and relative change of the damping force against the coil current for different frequencies (right).

the area under the force–displacement curve is increasing with rising current. Further on the clockwise tilting of the graph is remarkable. The increase of the enclosed area at higher currents can be explained with the increase of the fluid viscosity. The tilting seems to be caused by the elastic properties of the fluid.

In figure 13 (right side) the relative change of the damping force against the coil current is drawn. The measurements depicted were repeated for frequencies between 3 and 10 Hz. For each frequency the maximum damping force for coil currents from 0 A up to 2.5 A was measured. To make the results clearer the forces are normalized by subtraction of a certain amount of force to similar experiments without current. The results displayed in figure 13 show that the relative change of the damping force is increasing when the current is rising. Furthermore with increasing frequency the damping force is rising but the differences between the relative changes of the damping force get smaller with increasing frequency.

4.4. Conclusion and outlook

The concept of a magnetorheological damper based upon open porous metallic foams was realized and tested. The foam damper developed works with the flow mode. From the

measurement obtained it is obvious that on increasing the current of the magnetizing coil the damping force is rising. Measurements were carried out for various frequencies and coil currents. Regarding optimization issues there are some possibilities for increasing the damping force:

- Smaller open porosity of the metallic foam.
- A taller design space of the damper.
- Use of a magnetically controllable fluid with larger magnetized particles.

On using magnetically controllable fluids with large particles the problem of sedimentation appears. For applications where only small damping forces are required this can be solved by using nanomagnetorheological fluids or ferrofluids.

5. Summary and outlook

In this paper different applications featuring magnetically controllable fluids were introduced. The first one was the hydrostatic bearing with a magnetically controllable fluid. With this set-up it is possible to achieve quasi-infinite stiffness by the use of a suitable control strategy. The advantage of this system compared to conventional valve based systems is the quick response to payload changes. The second demonstrator which is described is a magnetohydrostatic bearing. It was shown that the idea of using ferrofluids in such a bearing is technically feasible. The potential of such bearings is in areas where only small bearing capacities are needed. Finally a new magnetorheological fluid damper with open porous foams was realized. This kind of damper has the advantage of reaching high damping forces in relation to a small design space.

Overall it can be concluded that magnetically controllable fluids offer high potential for various applications. To bring these demonstrators into technical application, in particular the properties of the magnetic fluids must be improved. For example, the bearing capacity of magnetohydrostatic bearing can be increased by ferrofluids with higher saturation limits. This could be realized either by the use of particle materials with higher magnetization saturation or by increasing the concentration of the ferrofluid particles.

References

- [1] Rowe W B 1983 *Hydrostatic and Hybrid Bearing Design* (London: Butterworth & Co.)
- [2] Tönshoff K 1995 *Werkzeugmaschinen: Grundlagen* (Berlin: Springer)
- [3] Spencer B F Jr, Dyke S J, Sain M K and Carlson J D 1997 Phenomenological model of a magnetorheological damper *J. Eng. ASCE* **3** 230–8
- [4] Bölter R 1999 *Design von Aktoren mit magnetorheologischen Flüssigkeiten* (Aachen: Shaker-Verlag)
- [5] Hesselbach J and Abel-Keilhack C 2002 Active hydrostatic bearing with magnetorheological fluid *Proc. 8th Int. Conf. on New Actuators* pp 343–6
- [6] Hesselbach J and Abel-Keilhack C 2003 Active hydrostatic bearing with magnetorheological fluid *J. Appl. Phys.* **93** 8441–3
- [7] Abel-Keilhack C 2004 *Magnetische Flüssigkeiten als Medium in hydrostatischen Lagern* (Essen: Vulkan-Verlag)
- [8] Lord Corporation 2003 Data sheet: Hydrocarbon-based MR fluid MRF-132AD www.rheonetic.com
- [9] Berkovsky B M 1993 *Magnetic Fluids, Engineering Applications* (Oxford: Oxford University Press)
- [10] Sproston J L, Yanyo L C, Carlson J D and El Wahed A K 2002 Controllable fluids in 2002-status of ER and MR fluid technology *Proc. 8th Int. Conf. on New Actuators (Bremen)* pp 333–8
- [11] Jolly M and Nakano M 1998 Properties and applications of commercial controllable fluids *Proc. 6th Int. Conf. on New Actuators (Bremen)* pp 414–9
- [12] Hesselbach J and Abel-Keilhack C 2004 Magnetorheologische Dämpfer 4. *Chemnitzter Produktionstechnisches Kolloquium* pp 473–84
- [13] Abel-Keilhack C 2004 Vorrichtung zum Übertragen von Kräften oder Momenten mit einem Arbeitsraum *Deutsches Patentamt Aktenzeichen* 102004024226.7